

Super-resolving Properties of Metallodielectric Stacks

Nkorni Katte¹, Joseph Haus¹, Jean-Bosco Serushema¹, Michael Scalora²

¹ Electro-Optics Program, University of Dayton, Dayton, OH 45469

² Charles M. Bowden Research Center, AMSRD-AMR-WS-ST, RDECOM, Redstone Arsenal, AL 35898-5000

Abstract

We show that diffraction can be suppressed in a realistic one-dimensional metallodielectric stack (MDS) at visible wavelengths to achieve super-resolution imaging. In our calculations we use two popular techniques, which can be adapted to investigate the imaging properties of MDSs. The two methods are the transfer matrix method (TMM) and the Finite element method (FEM) and they are compared with one another for consistency, when possible. We demonstrate the robustness and reliability of the full vector nature FEM without omitting the scattered fields and executed using appropriate boundary conditions. Our designs use material parameters taken from measured data and we use structures that can be achieved with the current state of art in nanofabrication technology. Calculations and experiments show that MDSs composed of periodic films, have a high signal throughput and are excellent candidates for widely tunable super-resolution devices.

1 Introduction

Optical transmission and replication of images is limited in resolution imposed by conventional

optical imaging systems to about $\lambda/2$. There have been many attempts to beat the diffraction

limit, which is contained in the sub-wavelength details of the image. The sub-wavelength details are carried by evanescent waves, which do not propagate in normal optical materials and instead, the field amplitudes exponentially decay in distance from the object plane.

In his 2000 PRL paper Pendry reported that imaging beyond the diffraction limit was possible with novel negative index materials (NIMs) because they restore the amplitude of the evanescent wave [1]. NIMs are materials with both negative dielectric permittivity and magnetic permeability and have been the subject of many papers over the past decade. In the same paper Pendry went on to propose that a metal, such as silver, with negative permittivity at optical and infrared frequencies will resolve sub-wavelength features [1].

Scalora et al showed that a multi-layer metallodielectric stack (MDS) could be used for high transmission, broadband super-resolution across the visible region. The simulated MDS consisted of silver (Ag) and Gallium Phosphide (GaP) layers that are designed for high transmission [2]. Super-resolution was found for the shorter wavelengths for TM polarization, while at longer wavelengths the super-resolution phenomenon became a highly channeled beam effect. For instance, light at 532nm wavelength passing through 40 nm wide apertures and

separated by a center-center distance of 120nm is predicted to be resolved at the sample's exit surface [3, 4].

The practical barriers to fabricating super-resolving devices are the surface roughness of the deposited films, and the experimental value of their optical constants. The measured optical constants vary significantly with fabrication parameters; sometimes a low-loss dielectric, which is often assumed in numerical simulations, will actually have high absorption after deposition. A material such as GaP is a good example of the difference between published and experimental data. In the literature it has a large dielectric constant and a wide band gap. However, when it is sputter deposited to form a thin film, its optical properties show higher losses due to stoichiometry changes. The process of fabricating low loss GaP is a continuing research effort.

For our calculations we consider using TiO₂ and GaP for the dielectric films. They both have relatively high indices and low losses across the visible regime and it has been sputter deposited with good, reproducible results. The metals, we have used in our study are Silver (Ag), Gold (Au) and Copper (Cu), see also [5]. The dielectric properties of Ag have been experimentally measured by several research groups recently, including researchers at the University of Dayton. We have compared two popular numerical techniques used to predict super-resolution for MDS. Our calculation confirms very well the theory that the TM polarized light is the appropriate choice for super-resolution. It also points the weakness of the TMM method, in revealing this detail. We have also demonstrated the possibility of super-guiding

within apertures of width $\lambda/10$ and super-resolve apertures with a pitch of $\lambda/5$.

2 Comsol Simulations

We have used FEM technique of COMSOL to calculate the transmission through several MDSs. We have also produced plots of channeled power through the MDS. We have calculated the cross sectional power at the image plane to determine the super-resolving capability of various MDSs.

Our FEM simulation shows that a MDS with thick dielectric layers of 80 nm will not be able to resolve the two 40nm wide aperture separated by a center to center distance of 160nm, a light of wavelength 650 nm is normally incident on the MDS. This result is different from that predicted by TMM. We conclude that our FEM, model rather predicts accurately and solve this problem in a very efficient way.

Comsol has also been used to address the nonlinear optical properties of a typical MDS discussed above. With it we have calculated the field and the phase at the exit layer of a MDS. This is usually the key task in the Z scan modeling in order to determine the nonlinear absorption coefficient and nonlinear refractive index of a material. Most Z scan simulations are performed with assumptions based on homogenous material, but our method addresses with great success this 1D photonic band gap structure.

3 Transmission and Super-resolving Regimes

In this section we show how both the TMM and COMSOL-based FEM give very similar results for the transmission properties of MDS when incident with TM polarized light at various wavelengths. The transmission being a very important property of the MDS will determine the applicability of MDS devices, for use in lithography or imaging of tiny biomolecules, optical limiting and optical switching.

We have considered several MDS designs, with dielectric properties of the metals taken from [5], while those of the dielectric are experimentally determined results. Blaikie et al. published a similar study on the transmission functions of MDS, which was based in the evanescent regime in which he compared TMM and COMSOL based FEM solutions [6]. Our study looks into more realistic cases of MDSs for super-resolution, which we think it is realized primarily because of the channeling of propagating waves [3, 4]. In this section, we shall examine the Transmission and resolving properties of two MDSs, denoted as MDS1 and MDS2.

First some general comments on the results presented below. In Figures 1a and 2a , we show the Transmission spectrum of the two designs we call: MDS1 and MDS2. Figures 1b and 2b are a comparison of the magnetic field squared for the FEM and TMM simulations. Figures 1c and 2c show the \log_{10} (Power flow) through MDS1 and MDS2 samples. Figures 1d , 2d and 3d , show the cross sectional irradiance plot at the exit layer of the each MDS.

3.1 MDS1

The first design which we call **MDS1** is described below. The design consists of 11 layers distributed as follows [GaP (20nm)/ 4.5 periods of Ag (20nm)/ GaP (30nm) /GaP (20nm)]. Its Transmission spectrum is shown in Figure 1a. The optical transmission peaks close to the wavelength of 550 nm at 45%. The structure of the magnetic field intensity, $|H|^2$, displays high penetration throughout the volume.

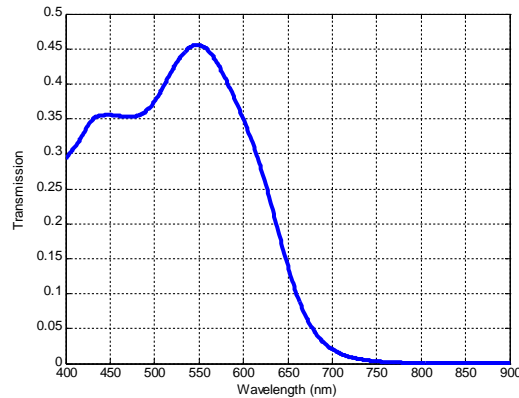


Figure 1a :Transmission spectrum of MDS1.

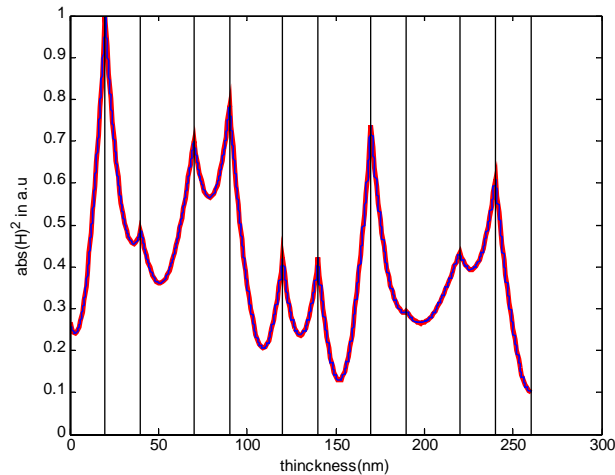


Figure 1b : Plot of the Magnetic field squared across the thickness of MDS1 consisting of Ag and GaP layers. There is an overlay of the red line over the blue line. The red line is the FEM simulation . While the blue line is TMM solution . Both methods give a transmission of 44% at an incident wavelength of 532nm.

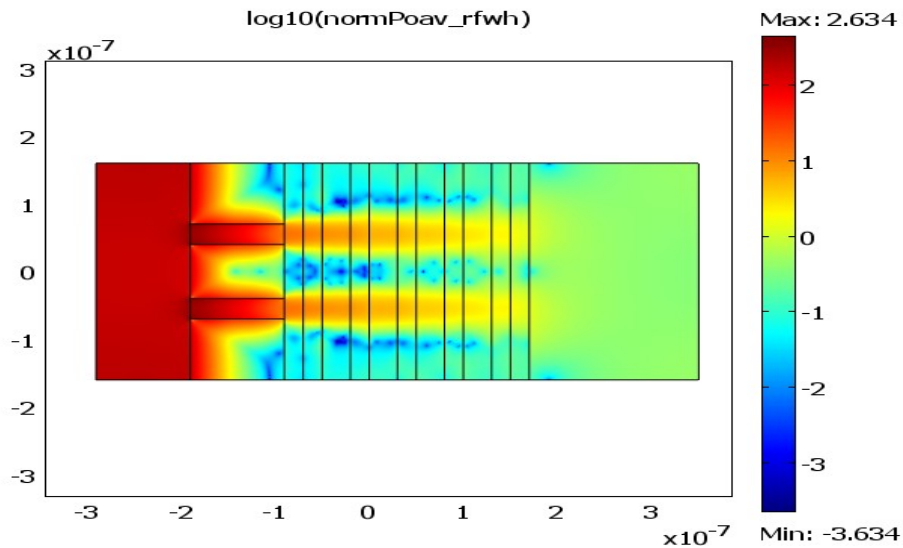


Figure 1c: The \log_{10} (Power) plot of the electromagnetic field propagating through two 30 nm slits separated by 110 nm at a wavelength of 532 nm.

The above picture in Figure 1c is showing the channeling of waves and resolution of two apertures incised on a Cr mask. The apertures are each 30nm wide and are separated by a center to center distance of 110nm. The whole structure is built on a glass substrate. A cross-section of the output irradiance is at the surface is shown in Figure 1d.

The Transmission at 532 nm is 0.4429. Both TMM code and COMSOL simulation gives the same result. The refractive index of GaP at 532 nm is taken as $n_{\text{GaP}}=3.2996-i*0.0384$, while that of Ag is $n_{\text{Ag}}=0.1301-i*3.1947$.

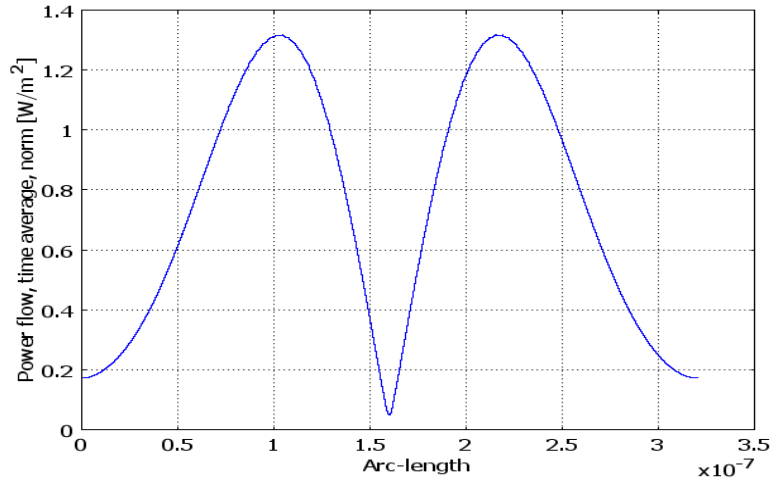


Figure 1d: Shows the cross section of the irradiance at the exit surface of MDS1. We notice the resolution of the two apertures inscribed on the mask.

3.2 MDS2

The second MDS, known here as MDS2 is made up of Au and GaP distributed as follows: [GaP (20nm)/3.5periods (Au (20nm)/GaP (30nm))/GaP (20nm)]. Its Transmission spectrum is shown below in Figure 2a. The comparison between the magnetic field intensities in Figures 1b and 2b shows how different the details can be.

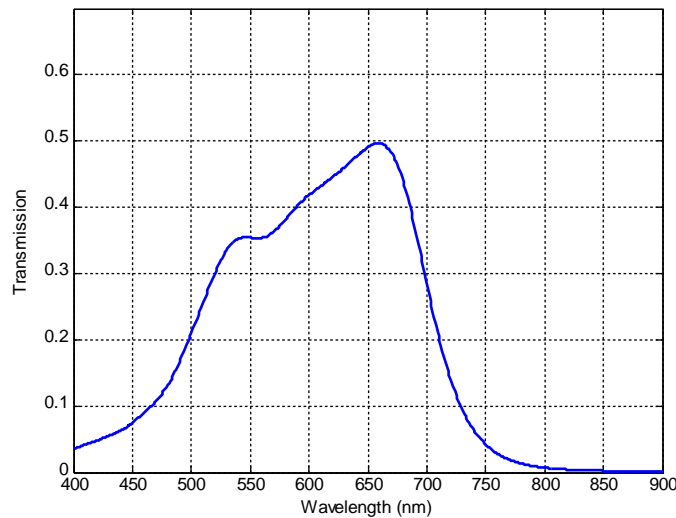


Figure 2a: Transmission spectrum of MDS2.

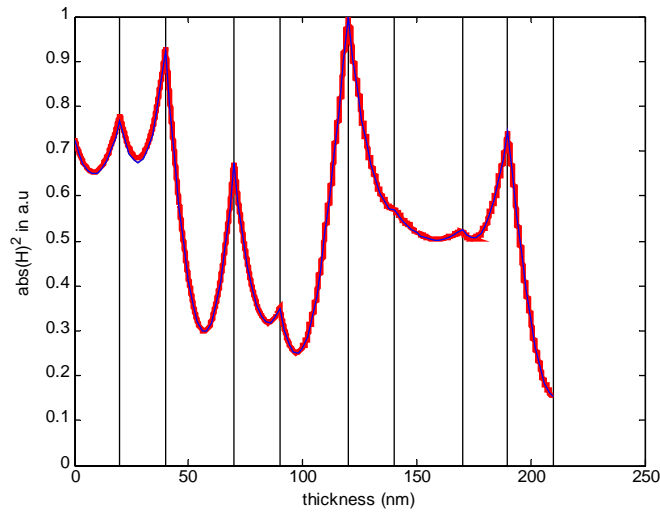


Figure 2b : Plot of the Magnetic field square across the thickness of MDS2 consisting of Au and GaP layers. There is an overlay of the red line over the blue line. The red line is the FEM simulation . While the blue line is TMM solution . Both methods give a transmission of 42% at an incident wavelength of 600nm.

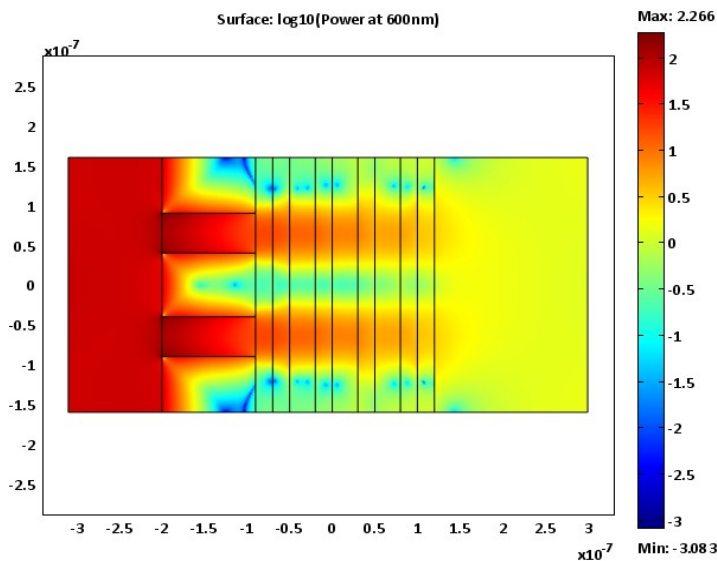


Figure 2c: The \log_{10} (Power) plot of the electromagnetic field propagating through two 50 nm slits separated by 100 nm at a wavelength of 600 nm.

The Transmission at 532 nm is 42% for both TMM code and COMSOL simulations. The refractive index of GaP at 600 nm is taken as $n_{\text{GaP}}=3.2405-i*0.0294$, while that of Au is $n_{\text{Au}}=0.2188-i*2.8625$. The results for transmission with two slits placed at the input are shown in Figures 2c and 2d, gain. The conclusions are similar to those in the previous section.

Figure 2d: Shows the cross section of the power at the exit surface of MDS2 We notice the resolution of the two 50nm wide apertures inscribed on the mask. The incident wavelength is 600 nm. The results above agree with the Scalora et al. results which identifies two regimes (i) a focusing regime at the edges of the pass band with no surface Plasmon excitation, and (ii) a beam

channeling, or super-guiding regime at the center of the pass band, as shown in Figure 2 for a transparent metal Ag/GaP structure, that favors the onset of transverse surface plasmons and super-resolution [4]. The MD photonic crystal structures are thicker than single metal layers; they contain more metal and have higher transmission. The focusing regime is prevalent at shorter wavelengths, near the edge of the pass-band. The output shows a focused spot at a standoff distance from the output plane. The channeling regime is apparent at longer wavelengths; the beam width in the MD structure can be maintained to a smaller fraction of a wavelength, but the features are eventually lost as the distance from the surface is increased.

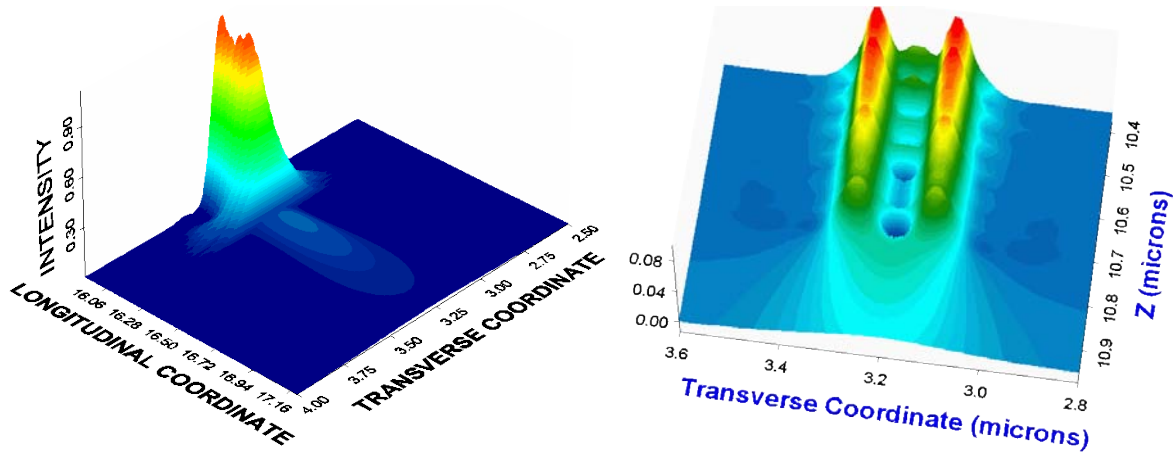


Figure 3: Transmission through a MD photonic crystal (the layers are parallel to the transverse coordinate) in the focusing regime, which shows the formation of an external focal spot (left), and in the super-resolving regime (right) showing the super-guiding regime, with two closely spaced $\lambda/20$ channels that do not interfere thanks to the formation of transverse Plasmon waves [4,7].

So far we have seen how both techniques give similar results of the transmission through MDS. We shall see further that the k-space based model of TMM even the Simple TMM model fails to take into account the whole spectrum of the transverse wave vector. Even though it accurately calculates the Transmission through the stack, its prediction about the super-resolving properties of the MDS is misleading.

3.4 Limitations of the standard TMM

In this subsection, we shall consider the limitation of the TMM in predicting super-resolution. We do so by considering a MDS, which we call MDS3 made up of 9 layers, with its layers distributed as: [TiO₂ (40nm)/ 3.5periods of (Cu (20nm)/TiO₂ (80nm)/TiO₂ (40nm)]. Consider a TM plane incident wave on a MDS3 [TiO₂ (40nm)/3.5periods of (Cu (20nm)/TiO₂ (80nm)/TiO₂ (40nm))] at 650nm. This stack will not be super-resolving because the thick dielectric layers will enhance diffraction and prevents the channeling which leads to super-resolution. However, if we use the TMM which gives us an intuitive picture of the propagation of this waves. It tells us that the two apertures separated by 160nm are completely resolved at the exit surface of the MDS as shown in Figure 4 below.

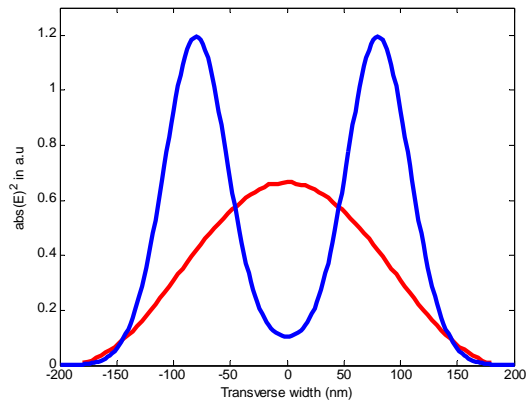


Figure 4: 1) Red line (FEM) shows that diffraction dominates and the two apertures cannot be resolved at the exit layer of MDS. 2) Blue line (TMM) Shows that the two apertures are resolved at the exit layer.

4 Nonlinear Photonics

Even though the super-resolving properties of MDS3 are not very promising, we take a look at its nonlinear absorption properties, which is important in the design of optical limiters. The Z scan technique is a common technique used to measure the optical nonlinearities of materials. The Z scan technique, developed by Bahae et al, involves moving a sample about the focus of a laser, beam, while measuring its transmission as a function of displacement. This is a very reliable technique, to measure the nonlinear absorption and nonlinear refraction [8].

We show here first the FEM, model solution for the Z scan experiment of a MDS. This model takes into consideration most of the involving physical interactions within the MD stack. It solves the corresponding nonlinear Maxwell's equation and provides us with the amplitude and the phase of the electromagnetic field at the exit layer of the MD stack. The standard Z- scan technique which has been used extensively to characterize several kinds of materials including a 1D photonic band gap device such as our MD stack usually ignores the losses due to internal multi-interference and back reflections, which contributes to the absorption within each layer [9]. Even when these phenomena are considered in the case of a bidirectional beam propagation method, transverse effects important in describing the beam profile are neglected [10]. These transverse effects are important for experimental purposes, since the power measured by the detector is the integral of the intensity of the beam over the area, captured by the profile of the beam. Even those who have included significant nonlinearity within some of the layers of the 1D photonic band gap stack in their model, often avoid solving the problem for realistic beams, but choose to address the nonlinear phase shift which can be easily calculated by assuming a plane wave incident [11, 12]. With The FEM approach we can consider a realistic input beam and define the physics of the problem to include all the back reflections, multi-interference within these thin layers of material, avoid using the slowly varying envelop approximation, which becomes difficult to manage for many contributing boundaries as in the case of a MDS [2]. The propagation of a Gaussian beam with a spot size of 20 microns at a wavelength of 650nm is shown in Figure 5 below. We assume a CW source; with COMSOL we extract the phase and the amplitude of the Electric field at the exit layer of MDS, which we numerically integrate by taking a Fourier transform to determine the electromagnetic field at the far field.

Figure 5: Showing the propagation of a Gaussian beam through a MDS. The result of an Open Aperture, FEM numerical Z scan experiment is presented below in Figure 6. For this simulation we introduced the nonlinearity within the metallic (Cu) layers only, since their nonlinear coefficients are a lot higher than those of the dielectric (TiO₂) layers. The nonlinear absorption coefficient, of the metal $\beta=4.75 \times 10^{-6} \text{cm}^2/\text{W}$, and the nonlinear refractive index $n_2=2 \times 10^{-11} \text{cm}^2/\text{W}$ were used [13].

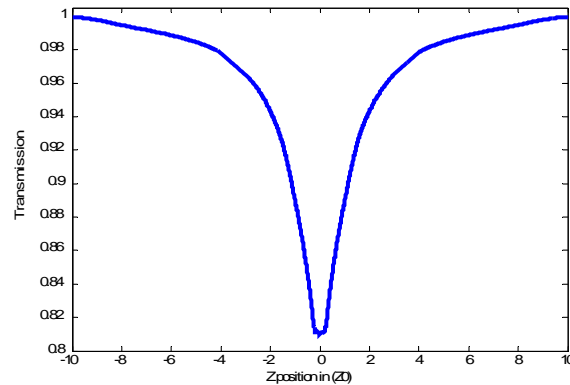


Figure 6: Z scan trace showing normalized transmission of a Cu/TiO₂ MD stack at an incident wavelength of 650nm. The layers of the stack are distributed as follows [TiO₂(40nm)/ 3.5 periods (Cu(20nm)/TiO₂(80nm)/TiO₂(40nm)].

5 Conclusions

We have shown how super-resolution is achieved at various wavelengths with MDS. We have compared the TMM and the FEM for Transmission, and Super-resolution. We find that even though both methods yield the same results for Transmission, the standard TMM method fails to accurately predict Super-resolution. We believe it is possible to modify the TMM, for it to accurately predict super-resolution.

Furthermore since we verified that the FEM can handle transverse effects, we have also simulated the propagation of a typical Gaussian beam through a nonlinear MDS. The output of this simulation has been used to model the standard CW Z scan experiment, and the results agree very well with the Z scan theory.

Acknowledgement: Nkorni Katte is grateful for financial support from the Graduate School at the University of Dayton.

References

[1] J. B. Pendry, "Negative refraction makes a perfect lens," Phys. Rev. Lett. **85**, 3966 (2000).

- [2] M. Scalora et al. "Negative refraction and sub-wavelength focusing in the visible range using transparent metallo-dielectric stacks," *Optics Express* **15**, 508-523 (2007).
- [3] M. J. Bloemer, G. D'Aguanno, N. Mattiucci, M. Scalora, and N. Akozbek, "Broadband super resolving lens with high transparency for propagating and evanescent waves in the visible range," <http://www.arxiv.org/abs/physics/0611162>.
- [4] D. de Ceglia, M. A. Vincenti, M. G. Cappeddu, M. Centini, N. Akozbek, A. D'Orazio, J. W. Haus, M. J. Bloemer, and M. Scalora, Tailoring Metallodielectric Structures for Super Resolution and Super guiding Application in the Visible and near IR Ranges, *Physical Rev. A* **77**, 033848 (2008).
- [5] E. D. Palik, *Handbook of Optical Constants of Solids* (Academic Press, New York, 1985).
- [6] C.P Moore, R. J. Blaikie, M. D. Arnold "An improved transfer-matrix model for optical superlenses", *Optics Express* **17**(16), 14260 (2009).
- [7] J.W. Haus, N. Katte, J. B. Serushema and M. Scalora, "Metallodielectrics as Metamaterials," "SPIE Optics and Photonics Conference, to appear (2010).
- [8] M. Sheik-Bahae, A. A. Said, T. Wei, D. J. Hagan, and E. W. Van Stryland, "Sensitive measurement of optical nonlinearities using a single beam," *IEEE J. Quantum Electron.* **26**, 760-769 (1990).
- [9] J. Wei and M. Xiao, "A Z-scan model for Optical nonlinear nanometric films," *Journal of Optics A, Pure Applied Optics* **10**,115102 (2008).
- [10] M. Scalora and M. Crenshaw, "A beam propagation method that handles reflections," *Optics Communication* **108**, 191-196, (1994).
- [11] S. Chen, W. Zang, A. Schuagen, X. Liu, J. Tian, J. Moloney and N. Peyghambarian, "Modeling of Z scan characteristics for one-dimensional nonlinear photonic band gap materials," *Optics Letters* **34**, 23 (2009).
- [12] R. Bennick, Y. Yoon, R. Boyd and J. Sipe, "Accessing the optical nonlinearity of metallo-dielectric photonic band gap structures," *Optics Letters* **24**, 20 (1999).
- [13] C. Hernandez, L. Padilha, J. Hales, D. Owens, J. Kim, S. Webster, S. Marder, J. Perry, D. Hagan, E. Stryland and B. Kippelen. *Integrated Photonics and Nanophotonics Research and Applications*, Honolulu Hawaii July 2009, Session (JTUA).